Molecular Therapy
Nucleic Acids
Original Article

Piezo 1 activation facilitates cholangiocarcinoma metastasis via Hippo/YAP signaling axis

Biqiang Zhu,[1] Wei Qian,[1] Chaoqun Han,[1] Tao Bai,[1,2] and Xiaohua Hou[1,2]

[1]Division of Gastroenterology, Union Hospital, Tongji Medical College, Huazhong University of Science and Technology, Wuhan 430022, China

Tumor metastasis is one of the major factors for the high mortality in cholangiocarcinoma (CCA), but its underlying mechanisms are not fully understood. Here, we report that Piezo-type mechanosensitive ion channel component 1 (Piezo 1) is detected to be significantly upregulated in CCA tissues, which is linked to a poor prognosis in patients, suggesting that Piezo 1 may act in a pro-metastatic role in CCA development. Piezo 1 is activated through 20% simulated physiological stretch, and deleting Piezo 1 impedes epithelial-to-mesenchymal transition (EMT) of CCA cells, as well as impairing their metastatic capacity *in vitro* and *in vivo*. Mechanistically, the activation of Piezo 1 results in large amounts of Yes-associated protein 1 (YAP) translocated into the nucleus from the cytoplasm, and thus the motility of CCA cells is significantly increased. These findings indicate that mechanical stimulation induces Piezo 1 activation, which might be involved in CCA metastasis via the Hippo/YAP signaling axis. Therefore, Piezo 1 and its downstream effectors may be a novel therapeutic target for CCA treatment.

INTRODUCTION

Cholangiocarcinoma (CCA) is a malignant tumor originated from bile duct epithelium with incidence and mortality increasing in recent years.[1] Local invasion or distant organ metastasis was noted in two-thirds of CCA patients when they received a confirmed diagnosis, missing the optimal time for surgical treatment.[2,3] The limited treatment options were confounded by a lack of understanding of how CCA cells acquire the capability to metastasize. Molecular-level details of the underlying causes of the metastatic cascade prior to spread are thus needed.

Metastasis, involving the spread to surrounding tissues and distant organs, is the primary cause of mortality.[4,5] It has been proven that the movement of cancer cells is precisely regulated by the mechanical microenvironment though a mechano-physiological pathway.[6,7] It is interesting that recent studies have emphasized the role of increasing interstitial fluid pressure (IFP) in metastasis.[8–10] Given that the high degree of mechanical stress caused by obstruction continuously stimulates CCA cells in tumor tissue formation, whether the stress is related to the CCA metastasis needs to be studied.

Piezo-type mechanosensitive ion channel component 1 (Piezo 1) is widely expressed in non-sensory tissues and cells under physiological conditions[11,12] and is a key sensor of the mechanical microenvironment. For example, Piezo 1 senses shear stress and cell volume in red blood cells and vascular endothelial cells and participates in the regulation of cell morphology and urine flow sensing.[13–15] Furthermore, an aberrant expression of Piezo 1 has been correlated with poor prognosis in some types of cancers in recent reports.[16–19] Interestingly, the role of Piezo 1 in cancer progression seems to be characterized by tissue dependence. Overexpression of Piezo 1 has been observed in a number of human cancers including breast cancer, bladder carcinoma, osteosarcoma, and gastric cancer, and knockdown of Piezo 1 attenuates adherence ability in these cancer cells, thus impeding cell metastasis,[19–21] whereas the situation in lung cancer is reversed, in that deletion of Piezo 1 accelerates lung cancer progression and cell migration.[22] To date, the role of Piezo 1 in CCA has not been investigated. The aim of this study was to determine whether Piezo 1 is involved in the development of CCA, especially tumor metastasis, and the possible mechanisms.

In the current study, several key issues have been addressed as follows: (1) to explore whether Piezo 1 acts as a major driver in CCA development, primary samples were analyzed at mRNA and protein levels, and functional studies were subsequently performed *in vitro* and *in vivo*; (2) to explore whether mechanical stretch is involved in CCA metastasis, a Flexcell system, modeling the mechanical stretch *in vitro*, was used; (3) to explore the main mechanobiological signaling axis involved in Piezo 1-mediated CCA metastasis, bioinformatics analysis was performed, and

Received 11 October 2020; accepted 22 February 2021;
https://doi.org/10.1016/j.omtn.2021.02.026.

[2]These authors contributed equally

Correspondence: Tao Bai, Division of Gastroenterology, Union Hospital, Tongji Medical College, Huazhong University of Science and Technology, 1277 Jiefang Avenue, Wuhan 430022, China.
E-mail: drbaitao@126.com
Correspondence: Xiaohua Hou, Division of Gastroenterology, Union Hospital, Tongji Medical College, Huazhong University of Science and Technology, 1277 Jiefang Avenue, Wuhan 430022, China.
E-mail: houxh@hust.edu.cn

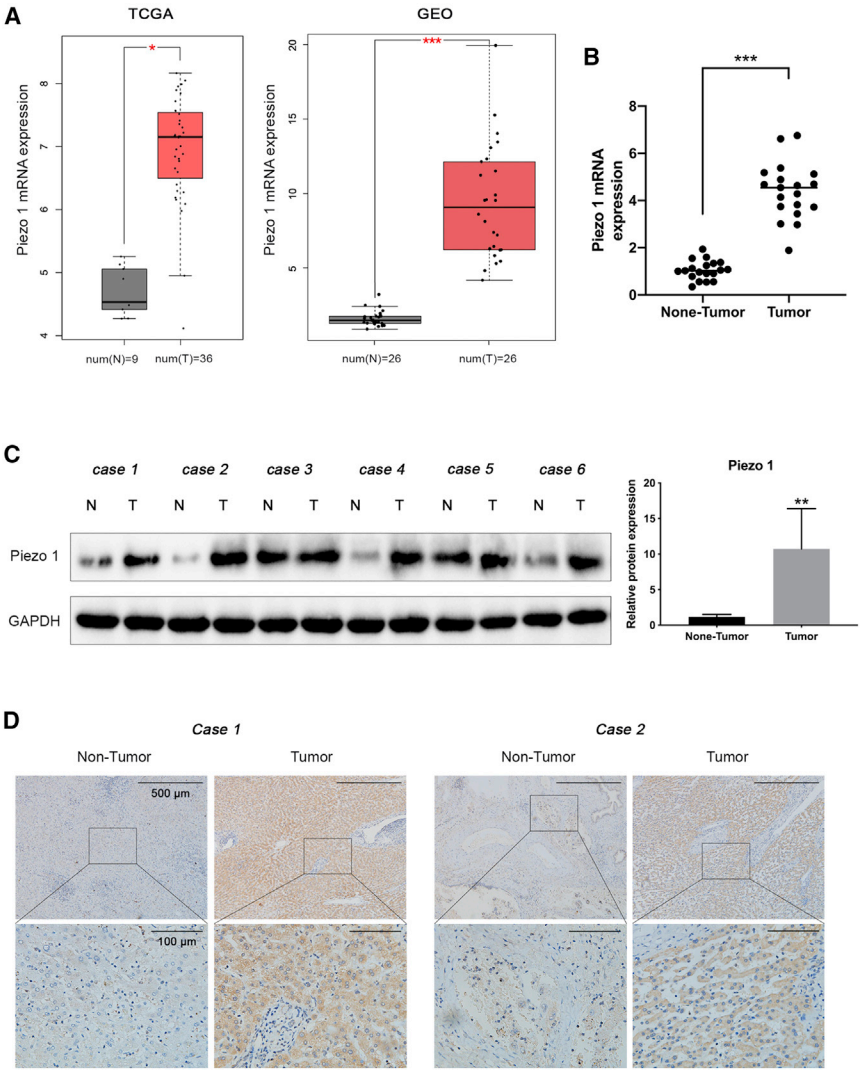

Figure 1. Piezo 1 is upregulated in human CCA tissues

(A) Piezo 1 mRNA levels in CCA tumor and non-tumor tissues analyzed using TCGA (https://www.cancer.gov/about-nci/organization/ccg/research/structural-genomics/tcga) and GEO (http://www.ncbi.nlm.nih.gov/geo/) databases. (B) Real-time PCR analyses of Piezo 1 mRNA levels in primary CCA tumor and non-tumor tissues. (C and D) Immunoblot and IHC analyses of Piezo 1 protein expression in CCA tissues and adjacent non-tumor tissues. Scale bars, 500 μm, 100 μm. Experiments were performed at least 3 times. *$p < 0.05$, **$p < 0.01$, ***$p < 0.001$.

further function studies were performed to verify the related pathways.

RESULTS

Upregulation of Piezo 1 is correlated with tumor metastasis and poor prognosis in patients with CCA

To determine the expression of Piezo 1 in CCA tissues, primary samples from the The Cancer Genome Atlas (TCGA) and GEO databases were first analyzed. Data showed that Piezo 1 was markedly increased in CCA tissues compared with the non-tumor tissues (Figure 1A). Furthermore, Piezo 1 in tumor tissues and adjacent tissues from CCA patients was also evaluated with real-time PCR, immunoblot, and immunohistochemical (IHC) analysis. As expected, Piezo 1 mRNA was significantly upregulated in tumor tissues compared with the non-tumor tissues (Figure 1B). Meanwhile, an increased expression of Piezo 1 was revealed in CCA tumor tissues compared with adjacent non-tumor tissues (Figures 1C and 1D).

Moreover, a clinicopathological characteristic analysis (including 9 cases from the TCGA database, 26 cases from the GEO database, and 19 cases who underwent surgical resection at the Union Hospital, Tongji Medical College, Huazhong University of Science and Technology between February 2018 and October 2019) indicated that the higher Piezo 1 expression is positively associated with tumor vascular invasion ($p = 0.014$) and distant metastasis ($p = 0.036$) (Table 1). Taken together, these results suggested that Piezo 1 may serve as a tumor promoter to facilitate the metastasis of CCA.

Deficiency of Piezo 1 reduces epithelial-to-mesenchymal transition (EMT) of CCA cells and inhibits metastasis

Given the positive association between Piezo 1 and vascular invasion and distant metastasis, CCA cell motility and invasiveness were tested after the endogenous Piezo 1 was stably knocked down by lentivirus transfection in TFK-1 and HuCCT-1 cells. To determine migratory ability, wound healing assays were performed; data showed that loss of Piezo 1 in CCA cells exhibited obvious delays in wound closure compared with the blank and negative control groups (Figure 2A). To further determine the motility and invasive behaviors, Transwell migration and invasion assays were performed. As expected, loss of Piezo 1 attenuated the migratory and invasive capabilities of TFK-1 and HuCCT-1 cells significantly (Figures 2B and 2C). Further study also demonstrated that deleting Piezo 1 induced cell apoptosis and impeded cell proliferation of TFK-1 and HuCCT-1 cells (Figures S1A and S1B).

Given that EMT is one of the hallmarks of elevated cell motility and metastasis,[23] expression of several EMT markers at mRNA and protein levels was tested. As shown in Figure 2D, knockdown of Piezo 1 upregulated the epithelial marker (E-cadherin) and suppressed the mesenchymal markers (N-cadherin and vimentin) in TFK-1 and HuCCT-1 cells. Together, these data indicated that

Table 1. Correlation between Piezo 1 staining and clinicopathological characteristics in CCA patients

Group		n	Piezo 1		p value
			Low	High	
Age (yr)	≤60	21	12	9	
	>60	33	15	18	0.402
Gender	male	23	11	12	
	female	31	16	15	0.783
CA 199 (U/mL)	≤37	20	11	9	
	>37	34	16	18	0.573
CEA (U/mL)	≤31	21	10	11	
	>31	33	17	16	0.78
Vascular invasion	no	29	19	10	
	yes	25	8	17	0.014*
Distant metastasis	no	44	25	19	
	yes	10	2	8	0.036*
Histological grading	well	19	12	7	
	medium/poorly	35	15	20	0.154

*Significant p value.

Piezo 1 induces the EMT program in CCA cells and promotes metastasis *in vitro*.

Deficiency of Piezo 1 suppresses CCA pulmonary metastases in mice

To validate the CCA metastatic effects of Piezo 1 knockdown *in vivo*, stable transfected cells were injected through the tail vein. Six weeks after injection, the mice in the Piezo 1 knockdown groups exhibited fewer and smaller lung metastatic nodules than the negative control groups (Figures 3A and 3B). The presence of the lung metastatic nodules was confirmed by hematoxylin and eosin (H&E) staining (Figure 3C). Immunoblot analysis of the lung tissues showed that the Piezo 1 knockdown-derived lung metastatic nodules had a relatively lower expression of N-cadherin and vimentin and higher expression of E-cadherin compared with the nodules from the negative control group (Figure 3D). Taken together, these results indicated that Piezo 1 induces the EMT program in CCA cells and promotes metastasis *in vivo*.

Mechanical stretch induces EMT in CCA cells via Piezo 1 activation

Given the obvious mechanical pressure in the bile duct after biliary obstruction caused by CCA tissues, a further study was performed to elucidate the role of mechanobiological mechanosensation signaling mechanisms in the development of CCA. We subjected the TFK-1 and HuCCT-1 cells to cyclic biaxial stretch with a Flexcell system. Cyclic stretch was kept at a continuous intensity and frequency (20% strain, 1 Hz), recapitulating the cardiac cycle, thus mimicking the forces experienced by CCA cells. TFK-1 and HuCCT-1 cells were treated with GsMTx4, a Piezo 1 channel inhibitor, or lentiviral transfection to inactivate Piezo 1 channel for 48 h. As Figure 4A shows, cells were observed to change in morphology from oval, polar, and closely connected to long and spindular with increased intercellular space in mechanical stretch groups, whereas Piezo 1 blockage with GsMTx4 incubation or Piezo 1 knockdown treatment reversed the changes by phase contrast microscopy. Immunofluorescence (IF) assays demonstrated that exposure to mechanical stretch resulted in lower fluorescence of the epithelial marker E-cadherin, whereas the blockage of Piezo 1 reversed the E-cadherin downregulation (Figure 4B). To further verify the EMT-related molecule changes, real-time PCR and immunoblot analysis were performed. As shown in Figures 4C and 4D, mechanical stretch upregulated the mesenchymal markers (N-cadherin and vimentin) and suppressed E-cadherin in TFK-1 and HuCCT-1 cells. In contrast, inactivation of Piezo 1 exhibited the opposite effects in TFK-1 and HuCCT-1 cells. Taken together, these results indicated that mechanical stretch induces CCA cell EMT through Piezo 1 activation.

Piezo 1 activation impedes Hippo signaling to activate YAP

To investigate the mechanisms underlying Piezo 1 activation-induced CCA metastasis, all the expression data of CCA tissues in the GEO and TCGA databases were downloaded with gdc-client and then organized into expression profiles. Genes with correlation greater than 0.3 or less than −0.3 and p value less than 0.05 were regarded as related genes, which were used for enrichment analysis. The KEGG pathway analysis showed that Hippo, transforming growth factor (TGF)-β, and HIF-1 signaling pathways were significantly altered upon Piezo 1 overexpression (Figure 5A).

To further confirm the molecules involved in the Piezo 1 activation-induced CCA cell EMT, TFK-1 and HuCCT-1 cells were treated with Yoda 1, a Piezo 1 agonist, and then immunoblot analysis was performed. Data showed that Smad 2/3, p-Smad 2/3, LATS 1, and HIF-1α expression was not significantly changed, whereas Piezo 1 activation in CCA cells indeed caused p-LATS 1 downregulation and Yes-associated protein 1 (YAP) upregulation. Surprisingly, p-YAP (Ser127), an indicator of YAP inactivation, was also increased (Figure 5B), which we assumed is due to the massive accumulation of total YAP. To verify this hypothesis, an equal amount of YAP extracted from each group was immunoprecipitated to measure p-YAP. As expected, decreased p-YAP was found after Yoda 1 treatment compared with the control (Figure 5C). Moreover, the expression of YAP target genes BIRC5 (survivin), CTGF, and CYR61 was upregulated at both mRNA and protein levels (Figures 5C and 5D), further supporting that Hippo signaling is repressed by Yoda 1 treatment. Consistently, upregulation of YAP target genes upon Piezo 1 activation implied that YAP might be translocated into the nucleus, which was confirmed by nucleus-cytoplasm fractionation (Figure 5E) and IF (Figure 5F).

Given the relevance between Piezo 1 and YAP described above, the expression of Piezo 1 and YAP in clinical tissues was analyzed. IHC

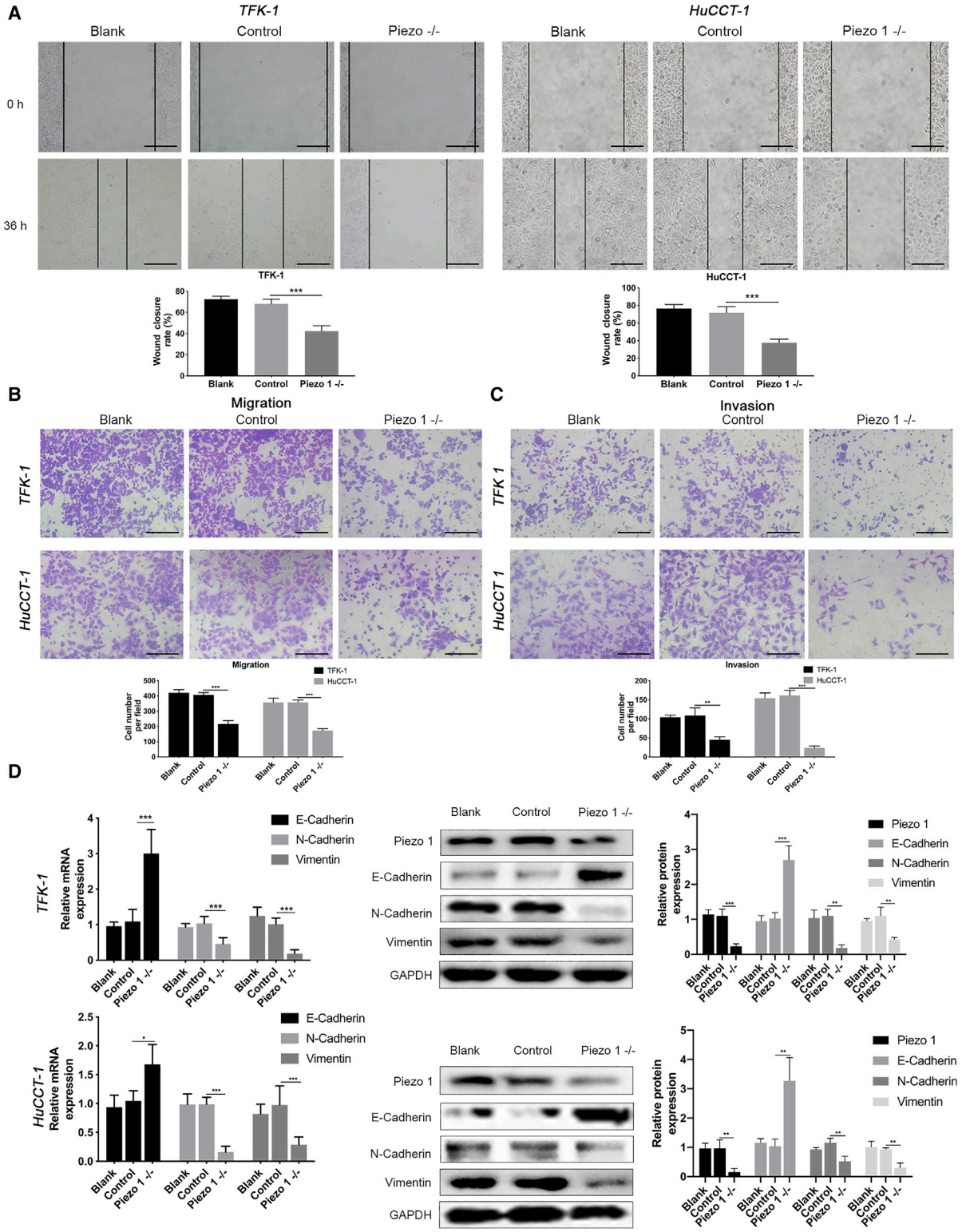

Figure 2. Deleting Piezo 1 suppresses CCA cell migration and invasion *in vitro*

(A) Cell migratory ability measured by wound healing assay. Scale bars, 200 μm. (B and C) Cell migration and invasive ability measured by Transwell and invasion assays. Scale bars, 200 μm. (D) EMT-related proteins analyzed by real-time PCR. Experiments were performed at least 3 times. *p < 0.05, **p < 0.01, ***p < 0.001.

A

Incidence of Lung Metastasis

Group	Lung Metastasis
TFK-1 Blank	4/5
TFK-1 Control	4/5
TFK-1 Piezo 1 -/-	2/5
HuCCT-1 Blank	5/5
HuCCT-1 Control	4/5
HuCCT-1 Piezo 1 -/-	2/5

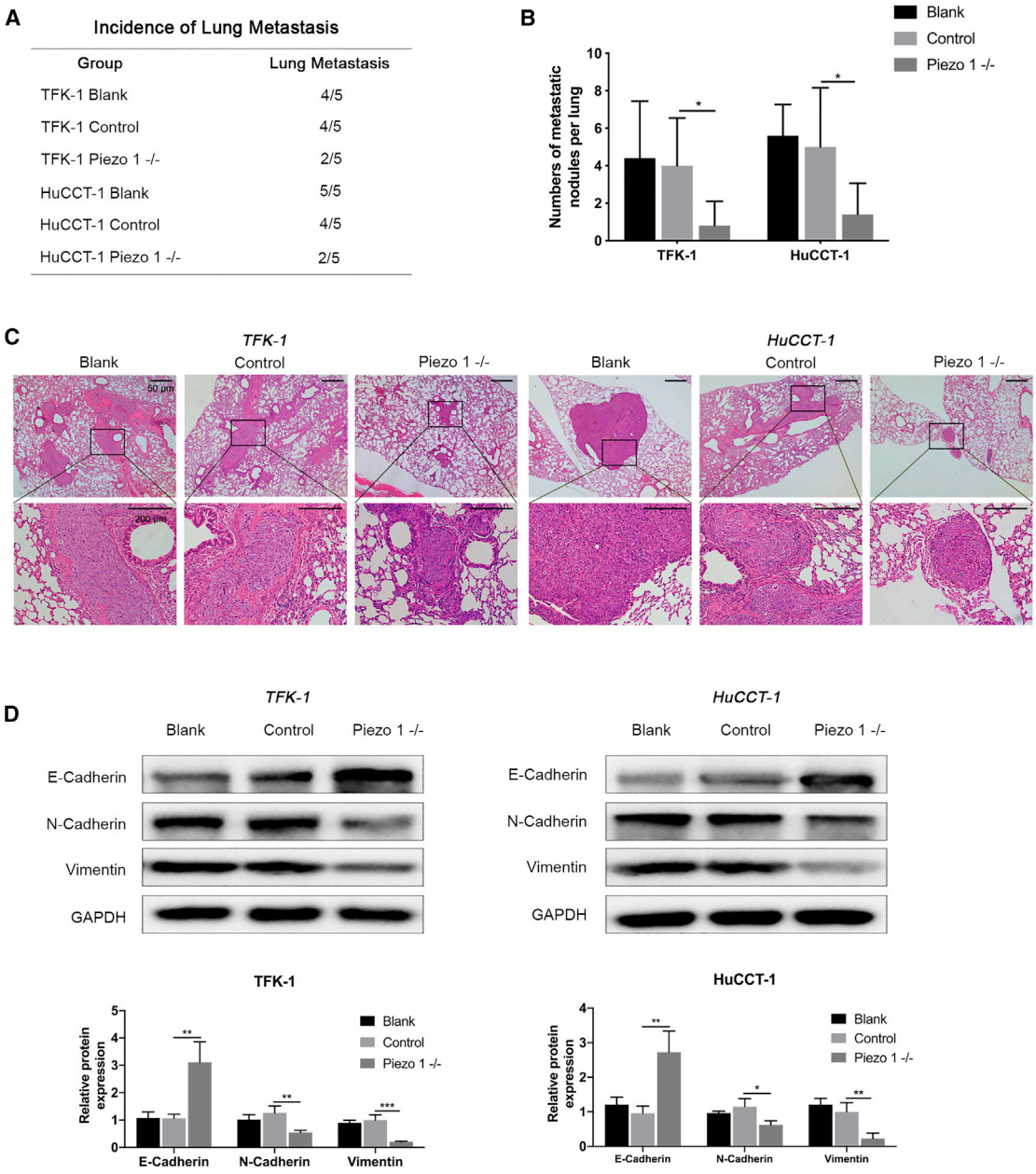

Figure 3. Piezo 1 promotes CCA lung metastasis in mice

(A and B) Lung metastasis of CCA in mice. (C) Metastatic nodules in the lungs of mice (40× magnification). Scale bars, 50 μm, 200 μm. (D) Protein levels of EMT-related molecules in metastatic nodules by immunoblot analysis. Experiments were performed at least 3 times. *p < 0.05, **p < 0.01, ***p < 0.001.

analysis supported that metastatic CCA tissues frequently showed high Piezo 1 levels and high YAP levels, whereas non-metastatic CCA tissues mostly exhibited low Piezo 1 expression and low YAP expression, indicating a positive correlation between Piezo 1 and YAP protein levels in CCA tissues (Figure 5G). Taken together, our results supported that the activated Piezo 1 protein impedes Hippo signaling, leading to the translocation of YAP into the nucleus, and targets the downstream genes.

Piezo 1 activation elevates CCA cell migration and invasion via YAP activation

Given that dysregulation of the Hippo signaling pathway promotes CCA development,[24,25] we proposed that YAP activation is required for increased cell migration and invasion induced by Piezo 1 activation. To test this hypothesis, cells were treated with Yoda 1 for Piezo 1 channel activation and incubated with or without verteporfin, a molecule able to block the formation of YAP/TEAD. After 48 h treatment,

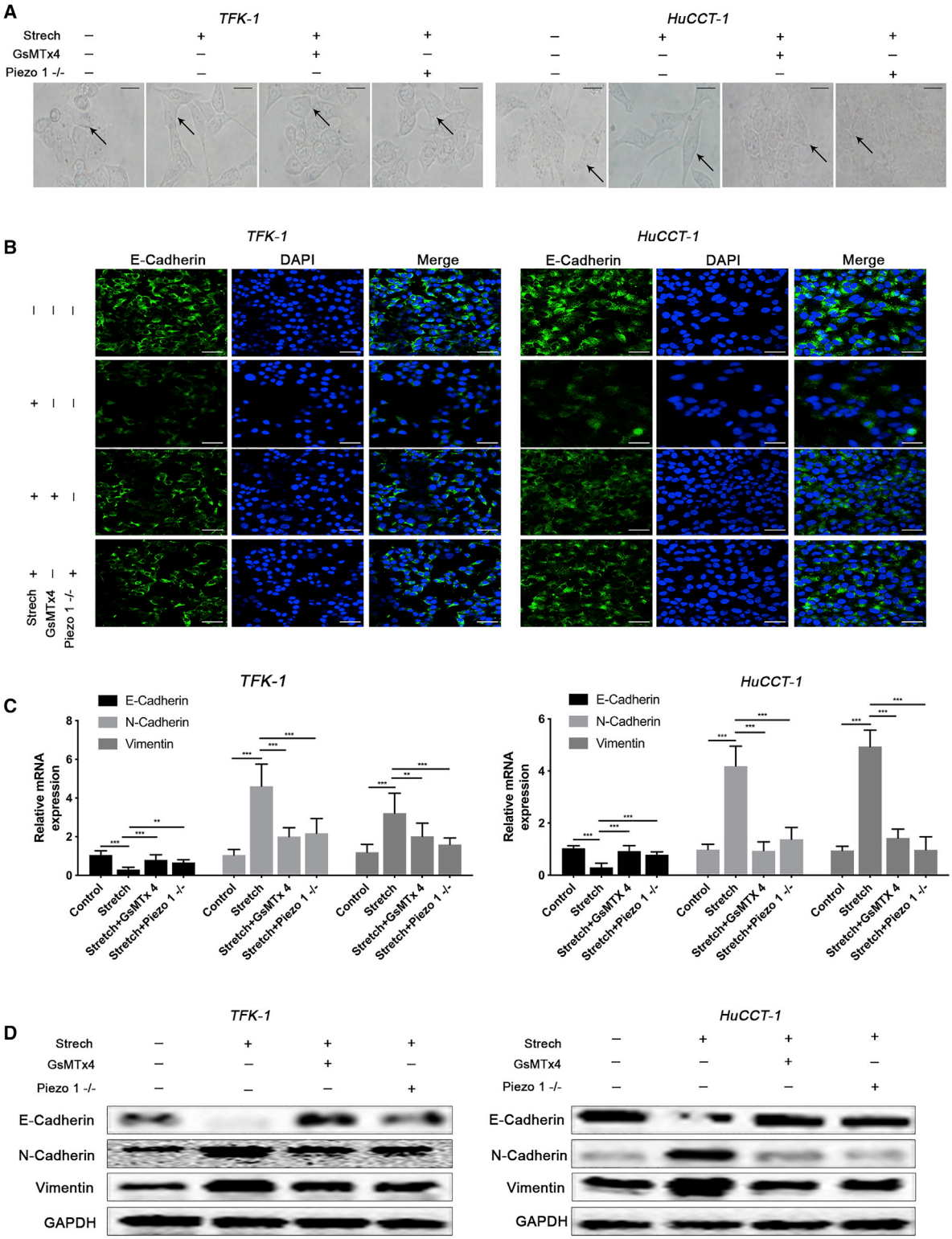

Figure 4. Mechanical stretch induces EMT in CCA cells

(A) Morphological changes of CCA cells. Scale bars, 10 μm. (B) IF analyses of E-cadherin expression. Scale bars, 50 μm. (C and D) mRNA and protein levels of EMT-related molecules measured by real-time PCR and immunoblot analysis. Experiments were performed at least 3 times. *p < 0.05, **p < 0.01, ***p < 0.001.

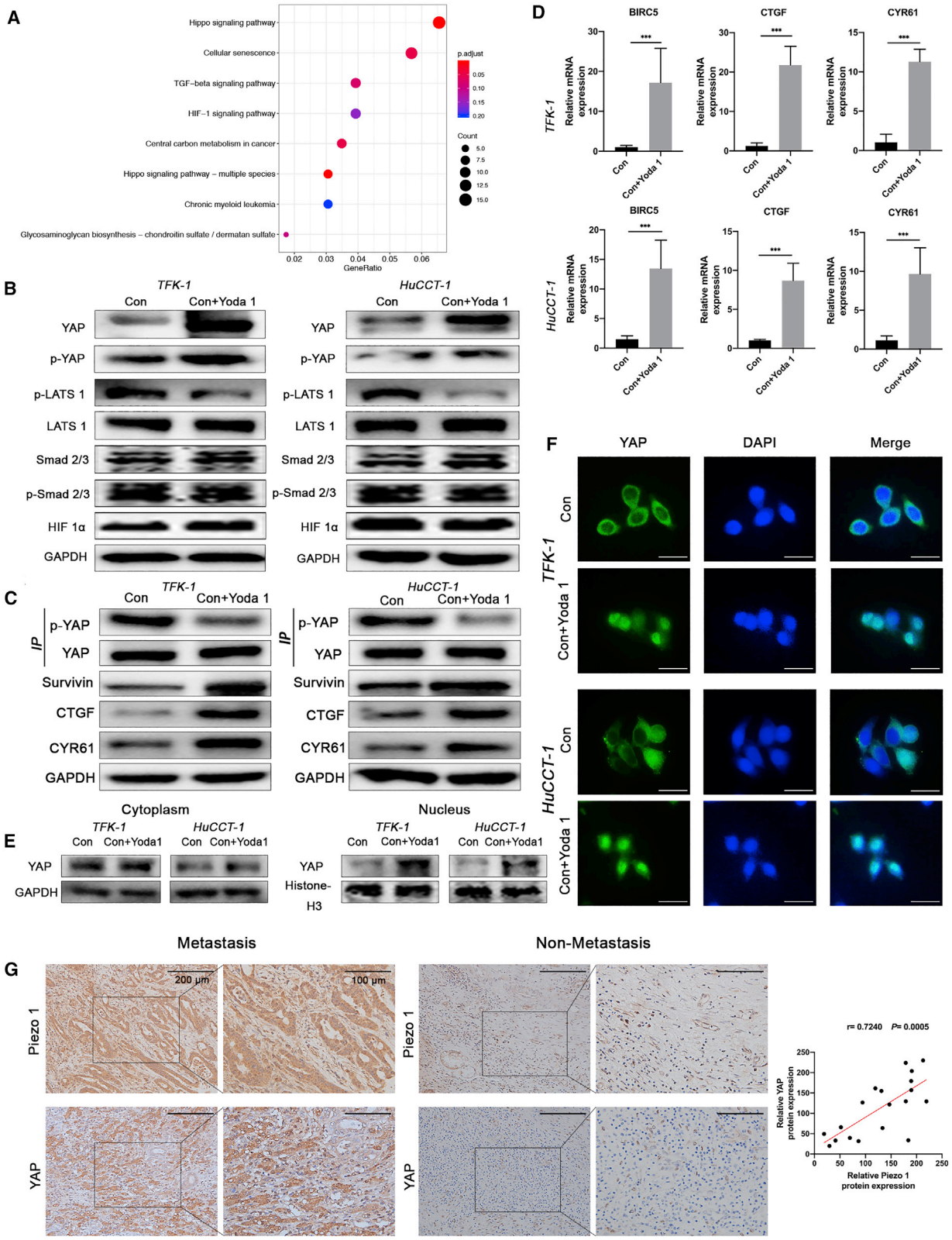

(legend on next page)

real-time PCR and immunoblot analysis implied that inhibition of YAP by verteporfin partially abrogated the Yoda 1-induced E-cadherin downregulation and N-cadherin and vimentin upregulation (Figures 6A and 6B). Furthermore, E-cadherin was marked and IF assay was performed; the data showed that after verteporfin treatment Yoda 1-induced E-cadherin fluorescence downregulation was reversed (Figure 6C). Moreover, inhibition of YAP by verteporfin partially abrogated CCA cell migration and invasion induced by Piezo 1 activation by Transwell migration and invasion assays (Figures 6D and 6E). Taken together, our data demonstrated that YAP activation is required for elevated CCA cell metastasis induced by Piezo 1 activation.

DISCUSSION

The accumulation of cholestasis caused by bile duct obstruction has been reported to induce dramatic changes in biliary tract pressure, altering biliary tract mechanobiology.[26,27] Given that the high degree of mechanical stress caused by obstruction continuously stimulates CCA cells in the case of tumor formation, whether the stress is related to the CCA metastasis needs to be studied. Here we showed that Piezo 1 was detected to be significantly upregulated in tumor tissues, which is linked to poor prognosis in patients with CCA. Moreover, the activated Piezo 1 was induced by mechanical force, leading to blockage of the Hippo signaling pathway, followed by the increased metastasis of CCA cells.

The present studies reveal that the expression of genes associated with EMT was differentially regulated by compression, supporting that this altered mechanical stretch in CCA increases the tendency towards metastasis. Although there was no direct evidence supporting that stress is associated with CCA development, it is reported that almost all cells are capable of sensing mechanical changes in the extracellular milieu and initiating appropriate responses to maintain tensional homeostasis by converting biomechanical force into biochemical signals and cellular responses, including physiological and neoplastic conditions. Sometimes, moreover, the effects are the opposite.[28,29] In theory, this drastic change in pressure can be sensed by all the cells in the medial side of the biliary tract, including the CCA cells. Our results demonstrated that the increased interstitial fluid pressure is related to the phenotypic and genotypic changes and enhances malignancy and tumor progression, providing the potential that relief of obstruction or bile drainage in CCA patients, such as endoscopic biliary stenting (EBS), endoscopic nasobiliary drainage (ENBD), percutaneous transhepatic biliary drainage (PTBD), and drugs for regulating Oddi sphincter function, may inhibit tumor metastasis. However, further clinical studies are needed to demonstrate the relationship between obstruction and metastasis.

In this study, Piezo 1 was found to be positively correlated with the metastasis of CCA *in vitro* and *in vivo*, which is consistent with reports that Piezo 1 activation promotes the development of many cancers, such as gastric cancer, glioma, and osteosarcoma. Interestingly, a recent study reported that loss of Piezo 1 accelerates non-small cell lung cancer progression and cell migration,[22] indicating that mechanical force-induced Piezo 1 activation may also act as an antioncogenetic factor in the development of certain cancer cells. It is suggested that different mechanical environments might be responsible for the opposite cell behaviors. Notably, recent studies revealed that mechanical stretch is more likely to induce cell division but not cell extrusion to death, whereas mechanical crowding exhibits the opposite effects.[16,30] Therefore, further studies are needed in the case of different types of mechanical intervention in CCA cells.

Another key finding in this study is the identification of the Hippo/YAP signaling pathway that is responsible for the Piezo 1 activation-induced CCA cell metastasis. Hippo signaling is an important signal transduction pathway originally discovered in *Drosophila* that is evolutionarily conserved to control organ size, working with a series of kinase cascades.[31,32] Malfunction of Hippo signaling leads to aberrant tissue growth and tumorigenesis.[33–36] The canonical Hippo pathway is composed of upstream kinases (MST1/2 and LATS1/2), nuclear transcription factors (TEADs), and transcriptional co-activator YAP. The phosphorylated MST1/2 activates LATS1/2, leading to the phosphorylation of the YAP/TAZ. Subsequently, the proteasomes in the cytoplasm ubiquitinate and degrade the phosphorylated YAP/TAZ, which controls organ size and tissue homeostasis. The compromised Hippo signaling results in various cancers including CCA.[37,38] Hippo kinase cascades can be regulated by other kinases, such as MAP4K, Mob, or TAO.[39–41] However, some proteins without kinase activity can indirectly modulate this kinase cascade. For example, Salvador has been reported to act as a scaffold connecting LATS1/2 and MST1, thereby promoting phosphorylation of LATS1/2.[42,43] Here, we report that Piezo 1 is a new Hippo regulator that is beneficial for LATS1 dephosphorylation, inhibiting Hippo signaling. Because of the lack of kinase activity, we hypothesize that Piezo 1 indirectly blocks LATS1 phosphorylation, which may be related to its cytoskeletal regulatory function. It is possible that the cytoskeleton may absorb some phosphatases to inhibit LATS1 phosphorylation, which needs more evidence. Moreover, a recent study reported that intracellular calcium levels contribute to tumor development through the Hippo pathway.[44] It is possible that the intracellular calcium activates certain phosphatases to repress LATS1 phosphorylation, which needs to be further explored.

Although we tried our best to improve the experiment, there are some deficiencies. The biological behaviors of cells after stretch intervention were not assessed in our study. This was mainly because mechanical stretch may affect the direction of cell movement in the process of

Figure 5. Overexpression of Piezo 1 inhibits Hippo/YAP signaling activation

(A) KEGG pathway was used for enrichment analysis, which was performed with the R package clusterProfiler. (B and C) Protein levels of related signaling pathways evaluated by immunoblot analysis. (D) mRNA levels of Hippo signaling components measured by real-time PCR. (E) Protein levels of YAP in cytoplasm and nucleus are shown. (F) Subcellular localization of YAP after Piezo 1 activation displayed by IF assay. Scale bars, 20 μm. (G) Correlation between Piezo 1 and YAP expression in CCA samples identified by IHC staining. Scale bars, 200 μm, 100 μm. Pearson correlation test; experiments were performed at least 3 times. ***$p < 0.001$.

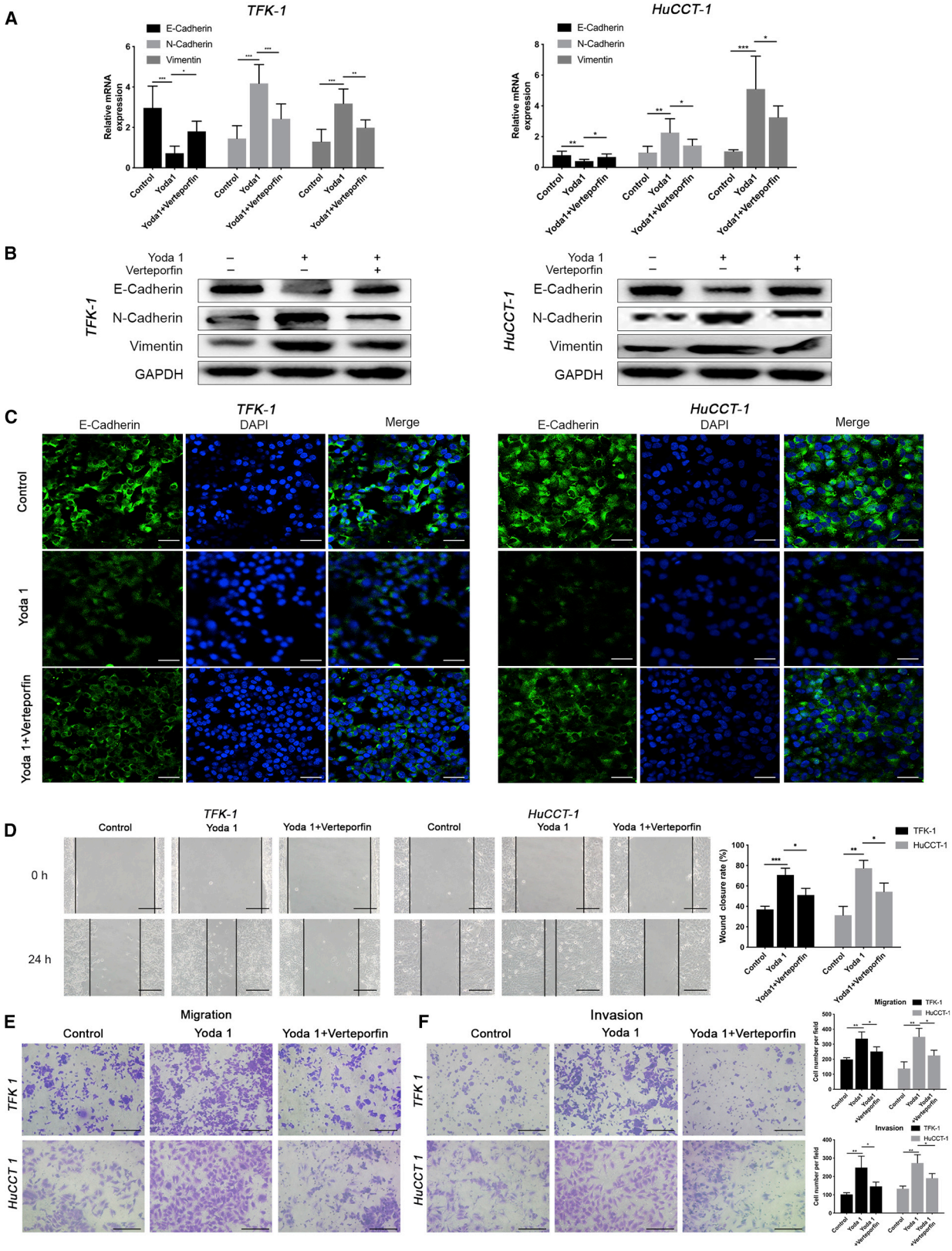

(legend on next page)

mechanical stimulation. More methods are needed to verify the changes of the movement ability of CCA cells under mechanical stretch treatment. In addition, our bioreactor cannot completely simulate the mechanical stress environment caused by the fluid in the biliary tract after the obstruction, but we will try to build an *in vivo* model to investigate the role of Piezo 1 in CCA.

In conclusion, the present study identified a significant association between aberrantly elevated Piezo 1 expression and poor prognosis in CCA patients. The Piezo 1 activation was induced by mechanical stretch, thus leading to the metastasis of CCA cells via the Hippo/YAP signaling axis. These results provide a foundation for understanding the mechanism of CCA development and support that Piezo 1 may serve as a promising prognostic and therapeutic target of human CCA.

MATERIALS AND METHODS

Patients, specimens, and cells

A total of 19 paired CCA tissues and adjacent tissues were collected from patients who underwent surgical resection at the Union Hospital of Huazhong University of Science and Technology between February 2018 and October 2019. All of the patients received no anti-tumor therapy before the surgery. CCA was staged according to the Cancer Staging Manual of the American Joint Committee on Cancer. A total of 35 paired sequencing results and clinical parameters of CCA samples were obtained from published databases (including 9 paired tissues from the TCGA database and 26 paired tissues from the GEO database). This study was approved by the Institutional Ethics Board of Union Hospital, Tongji Medical College, Huazhong University of Science and Technology. CCA cell lines, including TFK-1 and HuCCT-1, were maintained in RPMI 1640 medium supplemented with 10% fetal bovine serum (FBS) and 1% penicillin-streptomycin solution at 37°C in a 5% CO_2 atmosphere.

Reagents

The antibodies against E-cadherin (catalog no. 3159); N-cadherin (catalog no. 13116); vimentin (catalog no. 5741); YAP (catalog no. 14074); p-YAP (catalog no. 13008); Smad 2/3 (catalog no. 8685); HIF-1α (catalog no. 36169); LATS 1 (catalog no. 3477); p-LATS 1 (catalog no. 13008); survivin (catalog no. 2808); CTGF (catalog no. 86641); and CYR61 (catalog no. 14479) were purchased from Cell Signaling Technology (CST); antibody against p-Smad 2/3 (catalog no. ab272332) was purchased from Abcam; and antibody against Piezo 1 (catalog no. NBP1-78537) was purchased from Novus Biologicals. Verteporfin (YAP inhibitor, catalog no. HY-B0146) was purchased from MedChemExpress; GsMTx4 (Piezo 1 inhibitor, catalog no. ab141871) was purchased from Abcam. Yoda 1 (Piezo 1 agonist, catalog no. ab141871) was purchased from Abcam.

Lentivirus transfection

The lentiviral vector system (LV) and the empty vectors were purchased from GeneChem Corporation (Shanghai, China). Cells (5×10^5) were transfected with the specific virus at a multiplicity of infection of 20 in the presence of polybrene (6 μg/mL). After 12 h, the supernatant was replaced with cultured medium. Expression of Piezo 1 in transfected cells was validated by immunoblot analysis.

Immunoblot analysis

Cell and tissue proteins were lysed with RIPA buffer with protease and phosphatase inhibitors. Proteins were separated by sodium dodecyl sulfate-polyacrylamide gel electrophoresis (SDS-PAGE), and transferred to polyvinylidene fluoride (PVDF) membranes. The membranes were incubated with primary antibodies (1:1,000) at 4°C overnight and incubated with secondary antibodies (1:2,000) at room temperature for 2 h. After washing, the bounds were visualized with an enhanced chemiluminescence assay system.

Quantitative real-time PCR

Total RNA was extracted from cells or tumor tissues and subjected to reverse transcription to synthesize cDNA samples with a Total RNA Kit (Takara). SYBR Green Premix (Takara), cDNA, and primers were subjected to PCR amplification. GAPDH was used as internal control. Primer sequences are listed in Table S1.

IHC analysis

The tissue specimens were sliced, dewaxed, and hydrated. Tissue sections were placed in 3% hydrogen peroxide for 15 min, followed by placement on the slice holder and immersion in citric acid buffer solution for high-pressure repair for 5 min. Then, the tissue sections were placed in 10% goat serum and subsequently incubated with primary antibodies overnight. Then, the tissues were washed and incubated with the secondary antibody at room temperature for 1 h. Finally, the tissues were evenly dropped with DAB chromogenic solution.

Wound-healing assay

Cells were seeded in 6-well plates at 37°C in 5% CO_2 atmosphere until the cells grew to ~80% of the coverage area at the bottom. Two straight lines on the cell layer of each well were drawn with a 10 μL pipette tip. The treated 6-well plate was observed and photographed under a microscope.

Transwell migration and invasion assays

For the migration assay, 2.5×10^4 cells were seeded in the upper chambers of the Transwell containing FBS-free medium, and then the culture medium containing 10% FBS was added outside the chambers. For the Matrigel invasion assay, upper chambers were precoated with 30 μL of Matrigel for 6 h and the follow-up procedures were same as those for the migration assay. After incubation at 37°C under

Figure 6. YAP activation is required for elevated CCA cell metastasis induced by Piezo 1 activation

(A–C) EMT-related molecules of the cells after treatment with Yoda 1 or/and verteporfin measured by real-time PCR, immunoblot, and IF assays. Scale bars, 50 μm. (D and E) Cell migration and invasive ability measured by wound healing, Transwell, and invasion assays. Scale bars, 200 μm. Experiments were performed at least 3 times. *$p < 0.05$, **$p < 0.01$, ***$p < 0.001$.

an atmosphere of 5% CO_2 for the indicated hours, the non-migrating or non-invading cells remained on the upper surface of the filters. Cells that penetrated the membrane filters were fixed in methanol, stained with crystal violet, and counted under a light microscope.

Xenograft tumor-formation assay and treatment

Female BALB/c nude mice (Beijing Vital River Laboratory Animal Technology) aged 5 weeks were used in this study. For the *in vivo* metastasis assays, pulmonary metastases were established; 5×10^6 cells were injected into nude mice through the tail vein, and 6 weeks later tumor formation and metastasis in the lungs were measured. All the mice were euthanized, the lungs were excised, and the metastatic nodules were counted after H&E staining. All animal study protocols were approved by the Institutional Ethics Board of Union Hospital, Tongji Medical College, Huazhong University of Science and Technology.

Mechanical stretch system

Cells were seeded on 6-well plates with flexible silicone bottoms coated with collagen type IV (FLEXI culture plates). After incubation for 24 h, cells were subjected to cyclic stretch for 48 h. A strain amplitude of 20% was used at a rate of 60 cycles/min at 37°C and 5% CO_2 in a humidified incubator. The cells in the static group were not subjected to mechanical stretch and were placed in the same incubator next to the BioFlex loading station. Cyclic stretch was imposed at intensity and frequency (20% strain, 1 Hz) recapitulating the cardiac cycle, and therefore the forces experienced by CCA cells were mimicked.

Co-immunoprecipitation (coIP) assay

Cells were harvested and then lysed in 500 μL of coIP buffer containing a protease inhibitor cocktail (Sigma-Aldrich). After centrifugation, cell lysates were collected and precleared by incubating with 20 μL of immobilized protein A/G beads for 1 h at 4°C. The beads were then discarded with a magnetic frame and the lysates incubated with primary antibody or control immunoglobulin G (IgG) on a rotator at 4°C overnight. On the following day, 20 μL of immobilized protein A/G beads was added to precipitate the protein complex at 4°C for 4 h. Subsequently, samples were washed five times, the beads were boiled in loading buffer, and the proteins were prepared for immunoblot analysis as described above.

IF assay

The treated cells were fixed with 4% paraformaldehyde for 10 min, permeabilized with 0.1% Triton X-100 for 20 min at ambient temperature, blocked with 10% goat serum for 30 min, and then incubated with primary antibody overnight. The cells were washed and stained with goat anti-rabbit Alexa 488 secondary antibody at room temperature for 2 h. DNA staining was performed with DAPI. Confocal laser scanning microscopy was performed with a Leica TCSSP5 laser confocal microscope.

Statistical analysis

All data were analyzed with GraphPad Prism 8. Student's t test or one-way ANOVA analysis was used to evaluate statistical significance. Correlation was determined by Pearson correlation test. $p < 0.05$ was considered to indicate a statistically significant difference.

SUPPLEMENTAL INFORMATION

Supplemental information can be found online at https://doi.org/10.1016/j.omtn.2021.02.026.

AUTHOR CONTRIBUTIONS

B.Z., T.B., and X.H. designed this research. B.Z. performed most experiments in this work and drafted this manuscript. All authors read and approved the final manuscript.

DECLARATION OF INTERESTS

The authors declare no competing interests.

REFERENCES

1. Rizvi, S., Khan, S.A., Hallemeier, C.L., Kelley, R.K., and Gores, G.J. (2018). Cholangiocarcinoma - evolving concepts and therapeutic strategies. Nat. Rev. Clin. Oncol. *15*, 95–111.
2. Krasinskas, A.M. (2018). Cholangiocarcinoma. Surg. Pathol. Clin. *11*, 403–429.
3. Doherty, B., Nambudiri, V.E., and Palmer, W.C. (2017). Update on the Diagnosis and Treatment of Cholangiocarcinoma. Curr. Gastroenterol. Rep. *19*, 2.
4. Seyfried, T.N., and Huysentruyt, L.C. (2013). On the origin of cancer metastasis. Crit. Rev. Oncog. *18*, 43–73.
5. Robert, J. (2013). [Biology of cancer metastasis]. Bull. Cancer *100*, 333–342.
6. Northcott, J.M., Dean, I.S., Mouw, J.K., and Weaver, V.M. (2018). Feeling Stress: The Mechanics of Cancer Progression and Aggression. Front. Cell Dev. Biol. *6*, 17.
7. Munson, J.M., and Shieh, A.C. (2014). Interstitial fluid flow in cancer: implications for disease progression and treatment. Cancer Manag. Res. *6*, 317–328.
8. Gao, X., Zhang, J., Huang, Z., Zuo, T., Lu, Q., Wu, G., and Shen, Q. (2017). Reducing Interstitial Fluid Pressure and Inhibiting Pulmonary Metastasis of Breast Cancer by Gelatin Modified Cationic Lipid Nanoparticles. ACS Appl. Mater. Interfaces *9*, 29457–29468.
9. Mori, T., Koga, T., Shibata, H., Ikeda, K., Shiraishi, K., Suzuki, M., and Iyama, K. (2015). Interstitial Fluid Pressure Correlates Clinicopathological Factors of Lung Cancer. Ann. Thorac. Cardiovasc. Surg. *21*, 201–208.
10. Jain, R.K., Martin, J.D., and Stylianopoulos, T. (2014). The role of mechanical forces in tumor growth and therapy. Annu. Rev. Biomed. Eng. *16*, 321–346.
11. Solis, A.G., Bielecki, P., Steach, H.R., Sharma, L., Harman, C.C.D., Yun, S., de Zoete, M.R., Warnock, J.N., To, S.D.F., York, A.G., et al. (2019). Mechanosensation of cyclical force by PIEZO1 is essential for innate immunity. Nature *573*, 69–74.
12. Zhao, Q., Zhou, H., Chi, S., Wang, Y., Wang, J., Geng, J., Wu, K., Liu, W., Zhang, T., Dong, M.Q., et al. (2018). Structure and mechanogating mechanism of the Piezo1 channel. Nature *554*, 487–492.
13. Ge, J., Li, W., Zhao, Q., Li, N., Chen, M., Zhi, P., Li, R., Gao, N., Xiao, B., and Yang, M. (2015). Architecture of the mammalian mechanosensitive Piezo1 channel. Nature *527*, 64–69.
14. Friedrich, E.E., Hong, Z., Xiong, S., Zhong, M., Di, A., Rehman, J., Komarova, Y.A., and Malik, A.B. (2019). Endothelial cell Piezo1 mediates pressure-induced lung vascular hyperpermeability via disruption of adherens junctions. Proc. Natl. Acad. Sci. USA *116*, 12980–12985.
15. Andolfo, I., De Rosa, G., Errichiello, E., Manna, F., Rosato, B.E., Gambale, A., Vetro, A., Calcaterra, V., Pelizzo, G., De Franceschi, L., et al. (2019). *PIEZO1* Hypomorphic Variants in Congenital Lymphatic Dysplasia Cause Shape and Hydration Alterations of Red Blood Cells. Front. Physiol. *10*, 258.

16. Gudipaty, S.A., Lindblom, J., Loftus, P.D., Redd, M.J., Edes, K., Davey, C.F., Krishnegowda, V., and Rosenblatt, J. (2017). Mechanical stretch triggers rapid epithelial cell division through Piezo1. Nature *543*, 118–121.

17. Suzuki, T., Muraki, Y., Hatano, N., Suzuki, H., and Muraki, K. (2018). PIEZO1 Channel Is a Potential Regulator of Synovial Sarcoma Cell-Viability. Int. J. Mol. Sci. *19*, 1452.

18. Hashimoto, T., Ogawa, R., Yoshida, H., Taniguchi, H., Kojima, M., Saito, Y., and Sekine, S. (2019). EIF3E-RSPO2 and PIEZO1-RSPO2 fusions in colorectal traditional serrated adenoma. Histopathology *75*, 266–273.

19. Etem, E.O., Ceylan, G.G., Özaydın, S., Ceylan, C., Özercan, I., and Kuloğlu, T. (2018). The increased expression of Piezo1 and Piezo2 ion channels in human and mouse bladder carcinoma. Adv. Clin. Exp. Med. *27*, 1025–1031.

20. Li, C., Rezania, S., Kammerer, S., Sokolowski, A., Devaney, T., Gorischek, A., Jahn, S., Hackl, H., Groschner, K., Windpassinger, C., et al. (2015). Piezo1 forms mechanosensitive ion channels in the human MCF-7 breast cancer cell line. Sci. Rep. *5*, 8364.

21. Zhang, J., Zhou, Y., Huang, T., Wu, F., Liu, L., Kwan, J.S.H., Cheng, A.S.L., Yu, J., To, K.F., and Kang, W. (2018). PIEZO1 functions as a potential oncogene by promoting cell proliferation and migration in gastric carcinogenesis. Mol. Carcinog. *57*, 1144–1155.

22. Huang, Z., Sun, Z., Zhang, X., Niu, K., Wang, Y., Zheng, J., Li, H., and Liu, Y. (2019). Loss of stretch-activated channels, PIEZOs, accelerates non-small cell lung cancer progression and cell migration. Biosci. Rep. *39*, BSR20181679.

23. Pastushenko, I., and Blanpain, C. (2019). EMT Transition States during Tumor Progression and Metastasis. Trends Cell Biol. *29*, 212–226.

24. Marti, P., Stein, C., Blumer, T., Abraham, Y., Dill, M.T., Pikiolek, M., Orsini, V., Jurisic, G., Megel, P., Makowska, Z., et al. (2015). YAP promotes proliferation, chemoresistance, and angiogenesis in human cholangiocarcinoma through TEAD transcription factors. Hepatology *62*, 1497–1510.

25. Sugihara, T., Werneburg, N.W., Hernandez, M.C., Yang, L., Kabashima, A., Hirsova, P., Yohanathan, L., Sosa, C., Truty, M.J., Vasmatzis, G., et al. (2018). YAP Tyrosine Phosphorylation and Nuclear Localization in Cholangiocarcinoma Cells Are Regulated by LCK and Independent of LATS Activity. Mol. Cancer Res. *16*, 1556–1567.

26. Chung, B.K., Karlsen, T.H., and Folseraas, T. (2018). Cholangiocytes in the pathogenesis of primary sclerosing cholangitis and development of cholangiocarcinoma. Biochim. Biophys. Acta Mol. Basis Dis. *1864* (4 Pt B), 1390–1400.

27. Loeuillard, E., Fischbach, S.R., Gores, G.J., and Rizvi, S. (2019). Animal models of cholangiocarcinoma. Biochim. Biophys. Acta Mol. Basis Dis. *1865*, 982–992.

28. Butcher, D.T., Alliston, T., and Weaver, V.M. (2009). A tense situation: forcing tumour progression. Nat. Rev. Cancer *9*, 108–122.

29. Kao, Y.C., Lee, C.H., and Kuo, P.L. (2014). Increased hydrostatic pressure enhances motility of lung cancer cells. Annu Int Conf IEEE Eng Med Biol Soc *2014*, 2928–2931.

30. Xu, G.K., Liu, Y., and Zheng, Z. (2016). Oriented cell division affects the global stress and cell packing geometry of a monolayer under stretch. J. Biomech. *49*, 401–407.

31. Taha, Z., Janse van Rensburg, H.J., and Yang, X. (2018). The Hippo Pathway: Immunity and Cancer. Cancers (Basel) *10*, 94.

32. Misra, J.R., and Irvine, K.D. (2018). The Hippo Signaling Network and Its Biological Functions. Annu. Rev. Genet. *52*, 65–87.

33. Calses, P.C., Crawford, J.J., Lill, J.R., and Dey, A. (2019). Hippo Pathway in Cancer: Aberrant Regulation and Therapeutic Opportunities. Trends Cancer *5*, 297–307.

34. Qiao, Y., Li, T., Zheng, S., and Wang, H. (2018). The Hippo pathway as a drug target in gastric cancer. Cancer Lett. *420*, 14–25.

35. Salem, O., and Hansen, C.G. (2019). The Hippo Pathway in Prostate Cancer. Cells *8*, 370.

36. Ansari, D., Ohlsson, H., Althini, C., Bauden, M., Zhou, Q., Hu, D., and Andersson, R. (2019). The Hippo Signaling Pathway in Pancreatic Cancer. Anticancer Res. *39*, 3317–3321.

37. Sugihara, T., Isomoto, H., Gores, G., and Smoot, R. (2019). YAP and the Hippo pathway in cholangiocarcinoma. J. Gastroenterol. *54*, 485–491.

38. Ma, W., Han, C., Zhang, J., Song, K., Chen, W., Kwon, H., and Wu, T. (2020). The Histone Methyltransferase G9a Promotes Cholangiocarcinogenesis Through Regulation of the Hippo Pathway Kinase LATS2 and YAP Signaling Pathway. Hepatology *72*, 1283–1297.

39. Meng, Z., Moroishi, T., Mottier-Pavie, V., Plouffe, S.W., Hansen, C.G., Hong, A.W., Park, H.W., Mo, J.S., Lu, W., Lu, S., et al. (2015). MAP4K family kinases act in parallel to MST1/2 to activate LATS1/2 in the Hippo pathway. Nat. Commun. *6*, 8357.

40. Gundogdu, R., and Hergovich, A. (2019). MOB (Mps one Binder) Proteins in the Hippo Pathway and Cancer. Cells *8*, 569.

41. Tao, Y., Cai, F., Shan, L., Jiang, H., Ma, L., and Yu, Y. (2017). The Hippo signaling pathway: an emerging anti-cancer drug target. Discov. Med. *24*, 7–18.

42. Patel, S.H., Camargo, F.D., and Yimlamai, D. (2017). Hippo Signaling in the Liver Regulates Organ Size, Cell Fate, and Carcinogenesis. Gastroenterology *152*, 533–545.

43. Seo, E., Kim, W.Y., Hur, J., Kim, H., Nam, S.A., Choi, A., Kim, Y.M., Park, S.H., Chung, C., Kim, J., et al. (2016). The Hippo-Salvador signaling pathway regulates renal tubulointerstitial fibrosis. Sci. Rep. *6*, 31931.

44. Ma, X., Lu, J.Y., Moraru, A., Teleman, A.A., Fang, J., Qiu, Y., Liu, P., and Xu, T. (2020). A novel regulator of ER Ca^{2+} drives Hippo-mediated tumorigenesis. Oncogene *39*, 1378–1387.